TẠP CHÍ KHOA HỌC
TRƯỜNG ĐẠI HỌC QUY NHƠN

Tổng hợp vật liệu Co_3O_4 có nguồn gốc từ ZIF-67 và ứng dụng trong biến tính điện cực phát hiện acid ascorbic

Ngô Thị Thanh Hiền*, Nguyễn Vũ Ngọc Mai

Khoa Khoa học tự nhiên, Trường Đại học Quy Nhơn, Việt Nam

Ngày nhận bài: 09/04/2025; Ngày sửa bài: 25/06/2025
Ngày nhận đăng: 18/07/2025; Ngày xuất bản: 28/10/2025

TÓM TẮT

Trong nghiên cứu này, Co_3O_4 dạng tinh thể có cấu trúc xốp được tổng hợp bằng cách nung ZIF-67 trong môi trường không khí. Đặc trưng vật liệu Co_3O_4 được nghiên cứu bằng XRD, BET, SEM và EDS. Điện cực biến tính Co_3O_4-GPE dùng phát hiện điện hóa acid ascorbic thể hiện khoảng tuyến tính từ 2 µM đến 15 µM với giới hạn phát hiện là 0,48 µM. Kết quả độ thu hồi dao động từ 97,82% đến 99,5% đối với acid ascorbic xác định trong viên thuốc thương mại.

Từ khoá: *Co_3O_4, ZIF-67, acid ascorbic.*

**Tác giả liên hệ chính.*
Email: ngothanhhien@qnu.edu.vn

QUY NHON UNIVERSITY
JOURNAL OF SCIENCE

ZIF-67-derived Co_3O_4 porous crystalline material for electrochemical ascorbic acid detection

Ngo Thi Thanh Hien*, Nguyen Vu Ngoc Mai

Faculty of Natural Sciences, Quy Nhon University, Vietnam

Received: 09/04/2025; Revised: 25/06/2025
Accepted: 18/07/2025; Published: 28/10/2025

ABSTRACT

The Co_3O_4 porous crystalline material was synthesized by calcining ZIF-67 sample in air. The Co_3O_4 material was characterized by XRD, BET, SEM, and EDS. The electrode modified with Co_3O_4 was used to determine ascorbic acid. The proposed Co3O4-GPE electrode exhibited a linear range of 2 μM to 15 μM with a detection limit of 0.48 μM. Recovery results, ranging from 97.82% to 99.5%. for ascorbic acid in pharmaceutical tablet.

Keywords: *Co_3O_4, ZIF-67, ascorbic acid.*

1. INTRODUCTION

Ascorbic acid (AA), the common name for Vitamin C, is a common multivitamin component and occurs naturally in various foods.It is important for a healthy diet and acts as an antioxidant. However, an overdose of vitamin C can lead to side effects such as stomach upset, headache, difficulty sleeping, and skin flushing.[1,2] Therefore, the rapid and accurate determination of AA has attracted scientific attention.

Many analytical methods exist for determining ascorbic acid (AA), including techniques such as spectrofluorometry,[3,4] chromatography,[5,6] spectrophotometry,[7,8] capillary zone electrophoresis,[9,10] and electrochemistry.[11,12] Among these, electrochemical methods employing modified electrodes have received considerable interest owing to their inherent simplicity, high sensitivity, and economic viability.

Cobalt oxide is a semiconductor with wide applications in many fields, including catalysis, electrode materials, gas sensing, and drug delivery.[13-15] Numerous studies have explored the diverse applications of Co_3O_4; however, its potential use in electrode modification for pharmaceutical analysis remains relatively underexplored. To date, various porous nanostructures of Co_3O_4 have been synthesized, including spherical, tubular, rod-like, and flower-like morphologies. Most synthesis methods utilize cobalt carbonate or hydroxide salts as precursors, often yielding materials with relatively low surface areas.[16,17]

Recent, the application of metal-organic frameworks (MOFs; ZIFs) as precursors in the synthesis of inorganic materials is a growing area of research.[18-25] Studies show that heat treatment of ZIF-67 can pyrolyze their ligands and lead to the formation of metal oxide nanoparticles. Therefore, the metal-centered organic framework material Co (ZIF-67) has appeared as a potential precursor to synthesize cobalt oxide (Co_3O_4) while still inheriting the structural characteristics of ZIF-67 and improving its catalytic activity.

**Corresponding author.*
Email: ngothanhhien@qnu.edu.vn

https://doi.org/10.52111/qnjs.2025.19503

In this work, an electrode modified with the Co_3O_4 porous crystalline material derived from ZIF-67 is investigated. The obtained electrode was used for the electrochemical determination of AA.

2. EXPERIMENT

2.1. Chemicals

2-methylimidazol (2-Hmim, 98%), ascorbic acid, graphite powder and parafin oil were received from Sigma Aldrich. Cobalt nitrate hexahydrate [$Co(NO_3)_2 \cdot 6H_2O$, 99%] was purchased from Macklin (China). Phosphoric acid (H_3PO_4, 85%), potassium dihydrogen phosphate (KH_2PO_4, 99%), boric acid (H_3BO_3, 99%) and potassium hydroxide (KOH) were received from Guangdong-Guanghua Co. Ltd (China).

Vitamin C tablet (Vitamin C, 500 mg AA, from Pharimexco Viet Nam) was purchased from a local pharmacy. All chemical reagents were used as received without any further purification.

Britton-Robinson (B-R) buffer solutions were made using 0.5 M solutions of H_3BO_3, H_3PO_4, and CH_3COOH. The pH of the B-R buffer was adjusted to the desired value with 1 M KOH or 1M H_3PO_4 solutions.

2.2. Apparatus

All electrochemical analyses, including cyclic voltammetry and square wave voltammetry, were conducted using a DY2322 potentiostat, Digi-Ivy, Inc. Austin. A standard three-electrode cell was employed, consisting of a working electrode (Co_3O_4-GPE or bare GPE, 0.07 cm^2), a counter electrode (Pt wire), and a reference electrode (Ag/AgCl, KClsat).

2.3. Synthesis of Co_3O_4 porous crystalline material from ZIF-67

The synthesis of ZIF-67 was conducted according to a previously established method.[26]

1.455 g of $Co(NO_3)_2 \cdot 6H_2O$ was dissolved in 50 mL of ethanol, and 1.64 g of 2-methylimidazole (H_{mim}) was dissolved in 50mL of ethanol, resulting in a Co^{2+}: H_{mim} molar ratio of 1 : 4. The H_{mim} solution was slowly added to $Co(NO_3)_2$ solution under continuous stirring for 30 minutes at room temperature. The obtained mixture was allowed to stand at room temperature for 6 hours without stirring, leading to the formation of a colloidal dispersion. The solid product was collected by centrifugation (4000 rpm, 30 minutes), washed three times with ethanol, and dried at 80 °C, 12 hours.

The Co_3O_4 was obtained by calcining ZIF-67 in air at a heating rate of 1 °C·min−1.

2.4. Preparation of Co_3O_4-GPE modified electrode

To prepare the Co_3O_4-GPE modified electrode, 40 mg of graphite powder and 5 mg of Co_3O_4 powder were thoroughly mixed with 10 µL of paraffin oil. The resulting paste was then packed into a Teflon holder, and its surface was smoothed using paper. To renew the electrode surface, the outer 2 mm of paste was removed and replaced with freshly prepared paste.

2.5. Characterization of the Co_3O_4 porous crystalline material

A Bruker-Axs D8 diffractometer (40 kV, 40 mA) was used for powder XRD analysis. Textural properties were determined from nitrogen adsorption-desorption isotherms at -196 °C with a Micromeritics Gemini VII 2390 V1.02. Sample morphology was examined by scanning electron microscopy (JEOL JSM-6700F, 15 kV, 10 mA), and elemental composition was analyzed using EDS with a JSM-5700 LV.

3. RESULTS AND DISCUSSION

3.1. Characterization of the synthesized Co_3O_4 material

The XRD diffraction pattern of Co_3O_4 sample are shown in Fig. 1. The X-ray diffraction pattern exhibited reflections at 2θ values of approximately 31.5°, 36.8°, 38.0°, 44.6°, 55.8°, 59.4°, 65.3° and 77.5°, corresponding to the (220), (311), (222), (400), (422), (511), (440) and (533) crystalline planes of the Co_3O_4 cubic structure (JCPDS No. 04-043-1003)[25].

https://doi.org/10.52111/qnjs.2025.19503

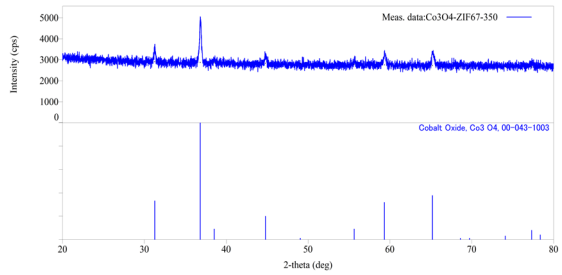

Figure 1. XRD pattern of the Co_3O_4 porous crystalline material.

The nitrogen adsorption-desorption isotherms were employed to characterize the specific surface area and pore morphology of the Co_3O_4 sample. As depicted in Figure 2, the sample presented a Type IV isotherm, accompanied by an H3 hysteresis loop, suggesting a mesoporous structure. The BET surface area was determined to be 30.43 m^2/g, and the pore size distribution was at 3 nm.

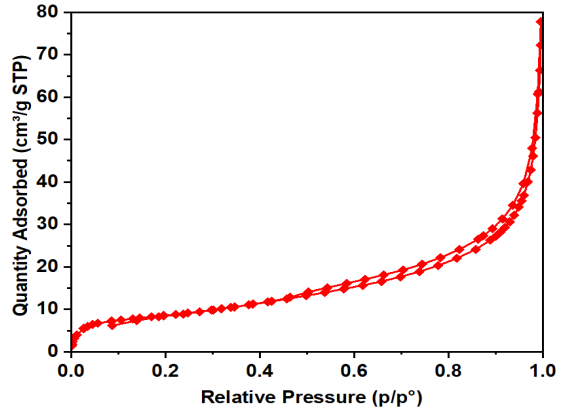

Figure 2. Nitrogen adsorption−desorption isotherms (A) and pore size distribution (B) of the Co_3O_4 porous crystalline material.

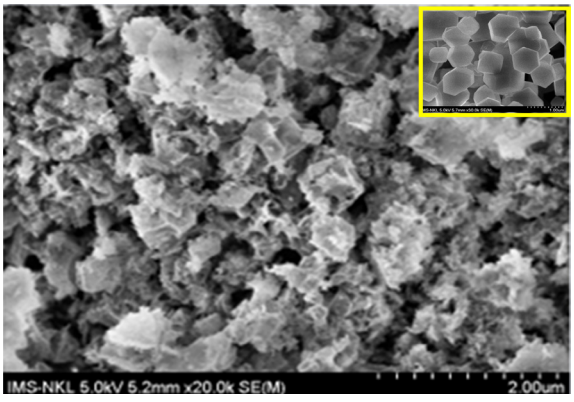

Figure 3. SEM image of the Co_3O_4 porous crystalline material, Inset: SEM image of ZIF-67 material.

The SEM images of Co_3O_4 (Figure 3) revealed that the calcined particles retained a cubic morphology, consistent with the original ZIF-67 crystal template, characterized by an internal hollow structure and a surface exhibiting porosity. However, thermal treatment resulted in the observation of some collapsed hollow structures.

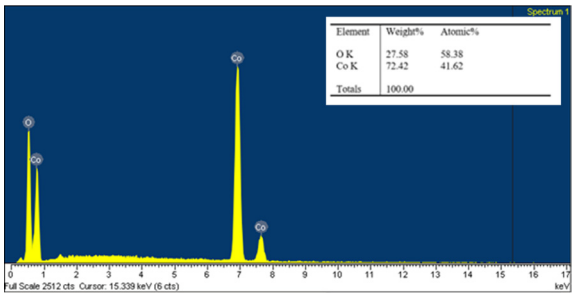

Figure 4. EDS spectra of the Co_3O_4 porous crystalline material.

The EDS analysis was conducted on the Co_3O_4 sample (Figure 4). Cobalt (Co) and oxygen (O) were confirmed to be present on the sample's surface based on the results. The elemental analysis of the Co_3O_4 yielded 41.62% cobalt and 58.38% oxygen.

A comprehensive morpho-structural analysis of the Co_3O_4 material, utilizing results of XRD, SEM, EDS and BET, validated the successful synthesis of the Co_3O_4 porous crystalline material.

3.2. Electrochemical characterization

The electrochemical behavior of ascorbic acid (AA) was investigated using cyclic voltammetry (CV) and square wave voltammetry (SWV).

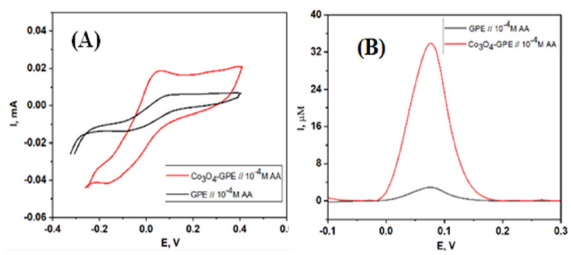

Figure 5. Cyclic voltammograms (A) and square wave voltammograms (B) at GPE and Co_3O_4-GPE modified electrode in 0.2 M B-R buffer solution pH = 4 containing of 10^{-4} M AA.

https://doi.org/10.52111/qnjs.2025.19503

A peak of AA at 0.08 V was observed in the CV and SWV curves obtained at both the bare GPE and the Co_3O_4-GPE, as illustrated in Figure 5. The Co_3O_4-GPE exhibited a lower peak potential and higher current. The oxidation peak current for AA at the Co_3O_4-GPE was approximately fifteen-fold greater than that observed at the bare GPE (Figure 5B) .

The reaction mechanism of ascorbic acid onto the Co_3O_4 nanostructure takes place by the transfer of two electrons and protons, as shown in Figure 6, and it has been generally represented in the literature [27, 28].

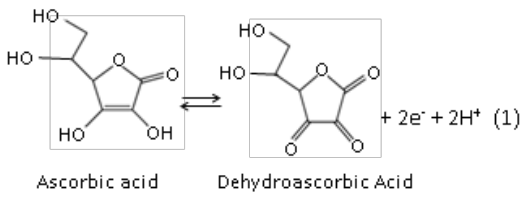

Figure 6. The electro-oxidation reaction of ascorbic acid.

Co_3O_4 showed catalytic activity for ascorbic acid electro-oxidation due to its unique redox properties, containing both Co^{2+} and Co^{3+} states. The catalytic process involves an electrochemical mechanism: surface Co^{3+} is electrochemically oxidized to a highly reactive Co^{4+}, which then chemically oxidizes ascorbic acid back to dehydroascorbic acid, regenerating Co^{3+}. This continuous regeneration ensures sustained catalytic activity. The porosity of Co_3O_4 derived from ZIF-67 further enhances its electrocatalytic performance. Its porous structure provides a large surface area with numerous active sites and facilitates efficient mass transport. This structure also improves the electrode-electrolyte interface and prevents nanoparticle agglomeration, significantly increasing the overall reaction rate and electrode efficiency.[29,30]

3.3. The effect of pH

The square wave voltammetry (SWV) was employed to examine the impact of pH (within the range of 3 to 6) on the voltammetric signals of AA. The pH of the electrolyte significantly affects the AA oxidation on the modified electrode. Figure 7 displays the current responses recorded on the Co_3O_4-GPE under different pH conditions.

A substantial increase in peak current was observed as t_{acc} increased from 0 to 90 seconds, suggesting a corresponding enhancement of AA accumulation at the electrode surface. Beyond 90 seconds, however, the peak current exhibited negligible increase, indicative of the electrode surface approaching adsorption equilibrium. Based on this observation, 90 seconds was selected as the optimal t_{acc}.

3.4. Accommulation

The effect of accumulation time (t_{acc}) on electrode response was investigated across a range of 0 to 150 seconds in a 0.2 M B-R buffer (pH 4) with 10^{-4} M AA (Figure 8).

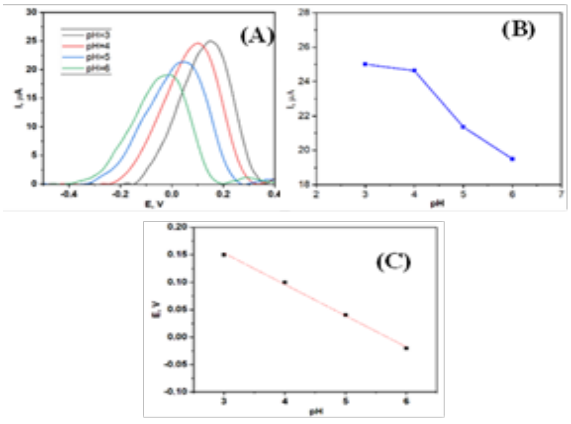

Figure 7. Square wave voltammograms of Co_3O_4-GPE in 0.2 M B–R buffer (pH 4) containing 10^{-4} M AA (A); Influence of pH on I_p (B); Plot of E_p vs. pH (C).

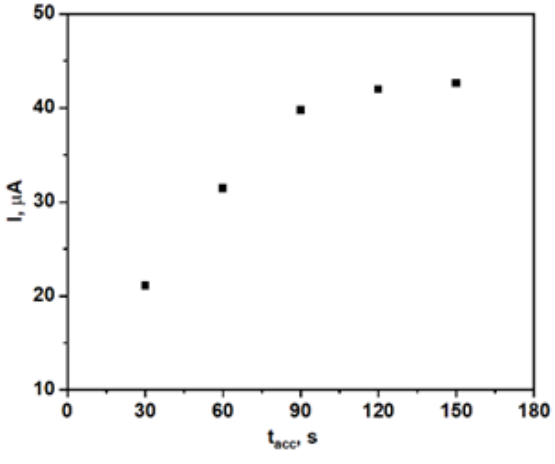

Figure 8. Dependence of I_p for AA in 0.2M B-R buffer solution pH 4 on accummulation time.

3.5. Calibration

The calibration curves for the AA detection with varying concentrations of AA was constructed by recording SWV in 0.2 M B-R buffer solution at pH = 4 (Figure 9A). Accordingly, a calibration curve was shown in Figure 9B. The electrode exhibited a linear response for AA concentrations between 2 µM and 15 µM.

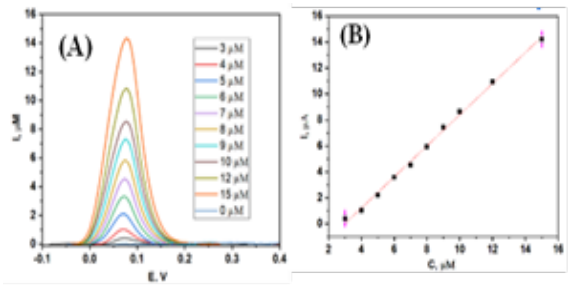

Figure 9. Square wave voltammograms recorded at Co_3O_4-GPE increasing concentration of AA (A) and the corresponding calibration curve (B).

The resulting linear regression equation was:

$$I_{pa}/\mu A = (-3.56335 \pm 0.19192) + (1.19706 \pm 0.02218)\ [AA]/\mu M,\ (R = 0.99726)$$

For ascorbic acid (AA) detection, the Co_3O_4-GPE electrode exhibited a 0.48 µM detection limit and a sensitivity of 1.19, which are lower compared to some published results (Table 1).

The continuous regeneration of the Co^{2+}/Co^{3+} redox couple in the investigated electrode increases the reaction rate, leading a larger current signal due to enhanced electron transfer. The resulting improved signal directly increases the electrode's sensitivity, allowing for the detection of even minor changes in analyte concentration. Consequently, the limit of detection (LOD) decreases, as a superior signal-to-noise ratio facilitates the reliable detection of very low analyte concentrations.

Table 1. Summary of electrode performance in this work and literature.

Electrode	Method	Detection limit, µM	References
CL-TiN/GCE	DPV	1.52	31
$NiCoO_2$/C	Amperometry	0.5	32
AgNP-Psi	Amperometry	0.83	33
GO-XDA-Mn_2O_3	DPV	0.6	34
rGO/Au/GCE	DPV	0.51	35
Co_3O_4-GPE	SWV	0.48	This work

3.6. Long-term stability and reproducibility

To assess the long-term stability, the electrode was stored at 4 °C in a refrigerator for 7 days, and the peak oxidation currents of 5µM AA in a 0.2 M B-R buffer solution were recorded. Measurements were conducted at various times. After 7 days of storage, the peak oxidation current of 5µM AA at the modified electrode retained 97.1% of its initial activity.

The reproducibility of the electrode's performance was determined. Three Co_3O_4-GPE electrodes were prepared independently following the same method. The measurements of their peak oxidation currents at 5µM AA showed consistent results, with a low RSD of 4.93%. This demonstrates that the Co_3O_4-GPE electrode has good reproducibility.

4. REAL SAMPLE ANALYSIS

The Co_3O_4-GPE electrode was used to analyze AA in Vitamin C tablets (Pharimexco Viet Nam) via the standard addition method to assess its applicability. Table 2 summarizes the results, confirming the electrode's effectiveness for AA determination in pharmaceuticals The measured mean AA concentration demonstrated agreement with the labeled value, and recovery rates ranged from 97.82% to 99.5%.

https://doi.org/10.52111/qnjs.2025.19503

Table 2. Results from the analysis of AA in a real Vitamin C tablet sample.

Sample	Added (μM)	Found (μM)	Recovery (%)	RSD (%)
Vitamin C (500 mg)	3	2.96 ± 0.02	98.66 ± 0.84	0.85

5. CONCLUSION

The synthesis of Co_3O_4 porous crystalline material was performed using the ZIF-67 material as a precursor. The resulting Co_3O_4 possesses an internal hollow structure and a surface exhibiting porosity. The modified electrode developed with Co_3O_4 porous crystalline material offers high sensitivity and a low detection limit, making it promising for AA detection. It has also been successfully used to determine AA in real samples.

Acknowledgements

This research is conducted within the framework of Science and Technology Projects at institutional level of Quy Nhon University under the project code T2024.832.03.

REFERENCES

1. M. Levine, Y. Wang, S. J. Padayatty, J. Morrow, A new recommended dietary allowance of vitamin C for healthy young women, *Proceeding of the National Academy of Science,* **2001**, *98*, 9842–9846.
2. C. M. Nam, K. W. Oh, K. H. Lee, S. H. Jee, S. Y. Cho, W. H. Shim, I. Suh, Vitamin C intake and risk of ischemic heart disease in a population with a high prevalence of smoking, *Journal of the American College of Nutrition,* **2003**, *22*, 372–378.
3. A. Jain, A. Chaurasia, K. K. Verma. Determination of ascorbic acid in soft drinks, preserved fruit juices and pharmaceuticals by flow injection spectrophotometry: matrix absorbance correction by treatment with sodium hydroxide, *Talanta*, **1995**, *42*, 779–787.
4. M. Tabata, H. Morita. Spectrophotometric determination of a nanomolar amount of ascorbic acid using its catalytic effect on copper(II) porphyrin formation, *Talanta,* **1997***, 44*, 151-157.
5. J. Lykkesfeldt. Determination of ascorbic acid and dehydroascorbic acid in biological samples by high-performance liquid chromatography using subtraction methods: reliable reduction with tris [2-carboxyethyl] phosphine hydrochloride, *Analytical Biochemistry,* **2000***, 282*, 89–93.
6. R. Thomis, E. Roets, J. Hoogmartens. Analysis of tablets containing aspirin, acetaminophen, and ascorbic acid by high-performance liquid chromatography, *Journal of Pharmaceutical Sciences,* **1984**, *73*, 1830–1833.
7. P. Ortega Barrales, M. L. F. d. Córdova, A. M. Dıaz. Indirect determination of ascorbic acid by solid-phase spectrophotometry, *Analytica Chimica Acta*, **1998**, *360*, 143-152.
8. M. Tabata, H. Morita. Spectrophotometric determination of a nanomolar amount of ascorbic acid using its catalytic effect on copper(II) porphyrin formation, *Talanta,* **1997***, 44*, 151–157.
9. W. S. Law, P. Kubáň, J. H. Zhao, S. F. Y. Li, P. C. Hauser. Determination of vitamin C and preservatives in beverages by conventional capillary electrophoresis and microchip electrophoresis with capacitively coupled contactless conductivity detection, *Electrophoresis*, **2005**, *26,* 4648–4655.
10. T. Wu, Y. Guan, J. Ye. Determination of flavonoids and ascorbic acid in grapefruit peel and juice by capillary electrophoresis with electrochemical detection, *Food Chemistry*, **2007**, *100*, 1573–1579.
11. Y. Zheng, H. Zhang, L. Fu. Preparation gold nanoparticles using herb leaf extract for electro-oxidation determination of ascorbic acid, *Inorganic and Nano-Metal Chemistry*, **2018**, *48*, 449-453.

12. A. Pardakhtya, S. Ahmadzadeha, S. Avazpoura, V. K. Gupta. Highly sensitive and efficient voltammetric determination of ascorbic acid in food and pharmaceutical samples from aqueous solutions based on nanostructure carbon paste electrode as a sensor, *Journal of Molecular Liquids,* **2016**, 216, 387–391.

13. X. Chen, J. Cheng, Q. Shou, F. Liu, X. Zhang. Effect of calcination temperature on the porous structure of cobalt oxide micro-flowers, *CrystEngComm,* **2012***, 14*, 1271-1276.

14. C. Sun, S. Rajasekhara, Y. Chen, J. B. Goodenough. Facile synthesis of monodisperse porous Co_3O_4 microspheres with superior ethanol sensing properties, *Chemical Communications*, **2011**, *48*, 12852-12854.

15. C. Sun, X. Su, F. Xiao, C. Niu, J. Wang. Synthesis of nearly monodisperse Co_3O_4 nanocubes via a microwave-assisted solvothermal process and their gas sensing properties, *Sensors and Actuators B: Chemical*, **2011**, *157*, 681-685.

16. R. He, H. Liang, C. Li, J. Bai. Enhanced photocatalytic hydrogen production over Co_3O_4@g-C_3N_4 p-n junction adhering on one-dimensional carbon fiber, *Colloids and Surface A: Physicochemical and Engineering Aspects*, **2020**, *586*, 124200.

17. H. Yu, J. Xu, Z. Liu. Functionalization of sheet structure MoS_2 with CeO_2–Co_3O_4 for efficient photocatalytic hydrogen evolution, *Jounal of Materials Science,* **2018***, 53*, 15271–15284.

18. Y. Y. Zheng, C. X. Li, X. T. Ding, Q. Yang, Y. M. Qi, H. M. Zhang, L. T. Q. Chin. Continuous synthesis for zirconium metal-organic frameworks with high quality and productivity via microdroplet flow reaction, *Chemistry Letters,* **2017***, 28,* 1473-1478.

19. M. Z. Hussain, Z. Yang, Z. Huang, Q. Jia, Y. Zhu, Y. Xia. Recent advances in metal–organic frameworks derived nanocomposites for photocatalytic applications in energy and environment, *Advanced Science*, **2021**, *14,* 2100625.

20. W. Li, X. Wu, N. Han, J. Chen, X. Qian, Y. Deng, W. Tang, Y. Chen. MOF-derived hierarchical hollow ZnO nanocages with enhanced low-concentration VOCs gas sensing performance, *Sensors and Actuators B: Chemical*, **2016**, *225*, 158–166.

21. K. Tao, X. Han, Q. Yin, D. Wang, L. Han, L. Chen, Metal-organic frameworks derived porous In_2O_3 hollow nanorod for high-performance ethanol gas sensor, *ChemistrySelect*, **2017**, *33*, 10918–10925.

22. Y. Cai, G. Fang, J. Zhou, S. Liu, Z. Luo, A. Pan, G. Cao, S. Liang. Metal-organic framework-derived porous shuttle-like vanadium oxides for sodium-ion battery application, *Nano Research*, **2018**, *11*, 449–463.

23. M. H. Yap, K. L. Fow, G. Z. Chen. Synthesis and applications of MOF-derived porous nanostructures, *Green Energy & Environment*, **2017**, *3*, 218–245.

24. C. Zhang, W. Chu, R. Jiang, L. Li, Q. Yang, Y. Cao, J. Yan. ZIF-67, derived hollow structured Co_3O_4 nanocatalysts: tunable synthetic strategy induced enhanced catalytic performance, *Catalysis Letters,* **2019**, *149*, 3058-3065.

25. X. Yan, L. Tian, M. He, X. Chen. Three-dimensional crystalline/amorphous Co/Co_3O_4 core/shell nanosheets as efficient electrocatalysts for the hydrogen evolution reaction, *Nano Letters Journal*, **2015**, *15*, 6015-6021.

26. T. T. H. Ngo, T. H. Y. Pham, N. T. Dang, T. V. H. Nguyen, T. H. Pham. Graziella liana turdean, graphite paste electrode modified with zeolitic imidazolate framwork (ZIF-67) for the determination of acetaminophen, *Studia UBB Chemia*, **2023**, *1*, 7-17.

27. K. Dhara, R. M. Debiprosad. Review on

nanomaterials-enabled electrochemical sensors for ascorbic acid detection, *Analytical Biochemistry,* **2019**, *586*, 113415.

28. A. M. Pisoschi, A. Pop, A. I. Serban, C. Fafaneata. Electrochemical methods for ascorbic acid determination, *Electrochimica Acta*, **2014**, *121*, 443-460.

29. N. Liu, M. Tang, C. Jing, W. Huang, P. Tao, X. Zhang, J. Lei, L. Tang. Synthesis of highly efficient Co_3O_4 catalysts by heat treatment ZIF-67 for CO oxidation, *Jounal of Sol-gel Science and Technology*, **2018**, 88, 163-171.

30. Y. Lu, W. Zhan, Y. He, Y. Wang, X. Kong, Q. Kuang, Z. Xie, L. Zheng. MOF-templated synthesis of porous Co_3O_4 concave nanocubes with high specific surface area and their gas sensing properties, *ACS Applied Materials & Interfaces*, **2014**, 6, 4186-4195.

31. L. Zhang, J. Feng, K. C. Chou, L. Su, X. Hou. Simultaneously electrochemical detection of uric acid and ascorbic acid using glassy carbon electrode modified with chrysanthemum-like titanium nitride, *Journal of Electroanalytical Chemistry,* **2017***, 803*, 11–18.

32. X. Zhang, S. Yu, W. He, H. Uyama, Q. Xie, L. Zhang, F. Yang. Electrochemical sensor based on carbon-supported $NiCoO_2$ nanoparticles for selective detection of ascorbic acid, *Biosensors and Bioelectronics,* **2014**, *55*, 446–451.

33. F. A. Harraz, M. Faisal, A. E. A. Salami, A. M. E. Toni, A. A. Almadiy, S. A. A. Sayari, M. S. A. Assiri. Silver nanoparticles decorated stain-etched mesoporous silicon for sensitive, selective detection of ascorbic acid, *Materials Letters*, **2019**, *234*, 96-100.

34. A. Ejaz, S. Jeon. A highly stable and sensitive GO-XDA-Mn_2O_3 electrochemical sensor for simultaneous electrooxidation of paracetamol and ascorbic acid, *Electrochimica Acta,* **2017**, 245, 742–751.

35. C. Wang, J. Du, H. Wang, C. E. Zou, F. Jiang, P. Yang, Y. Du. A facile electro chemical sensor based on reduced graphene oxide and Au nanoplates modified glassy carbon electrode for simultaneous detection of ascorbic acid, dopamine and uric acid, *Sensors and Actuators B: Chemical*, **2014**, *204*, 302–309.